

Supporting Information

Noble-metal-free NiFeMo nanocatalyst for hydrogen generation from the decomposition of a hydrous hydrazine solution

Hong-Li Wang, Jun-Min Yan, Si-Jia Li, Xue-Wei Zhang, and Qing Jiang*

Key Laboratory of Automobile Materials, Ministry of Education, Department of Materials Science and Engineering, Jilin University, Changchun 130022, China.

Chemicals: Hydrazine monohydrate ($\text{H}_2\text{NNH}_2 \cdot \text{H}_2\text{O}$, Sinopharm Chemical Reagent Co., Ltd, 85%), nickel (II) chloride hexahydrate ($\text{NiCl}_2 \cdot 6\text{H}_2\text{O}$, Sinopharm Chemical Reagent Co., Ltd, >98%), iron (II) sulfate heptahydrate ($\text{FeSO}_4 \cdot 7\text{H}_2\text{O}$, Sinopharm Chemical Reagent Co., Ltd, >99%), sodium molybdate dihydrate ($\text{Na}_2\text{MoO}_4 \cdot 2\text{H}_2\text{O}$, Sinopharm Chemical Reagent Co., Ltd, >99%), sodium borohydride (NaBH_4 , Sinopharm Chemical Reagent Co., Ltd, >96%), sodium hydroxide (NaOH , Beijing Chemical Works, >96%) were used without further purification. De-ionized water with the specific resistance of $18.2 \text{ M}\Omega \cdot \text{cm}$ was obtained by reversed osmosis followed by ion-exchange and filtration.

Physical Characterizations: Powder X-ray diffraction (XRD) measurements were performed on a Rigaku D/max-2500 X-ray generator with Cu $K\alpha$ radiation ($\lambda=1.54056 \text{ \AA}$). Transmission electron microscope (TEM, JEM-2100F, JEOL, 200kV) and corresponding energy-dispersive X-ray (EDX) were applied to analyze microstructures and compositions of the samples, and the amorphous carbon coated copper grids were used as the sample supporters. X-ray photoelectron spectroscopy (XPS) spectra were acquired after Ar sputtering for 15 min with an ESCALABMKLL (Vacuum Generators) spectrometer using Al $K\alpha$ X-rays (240 W).

Mass spectrometry (MS) analysis of the generated gas was performed using an

OmniStar GSD320 mass spectrometer, wherein Ar was chosen as the carrying gas. UV-vis absorption spectra were recorded on an Agilent Cary 50 spectrophotometer in the wavelength range of 390-700 nm.

Syntheses of catalysts: The $\text{Ni}_{0.6}\text{Fe}_{0.4}\text{Mo}$ nanoparticles (NPs) was prepared through a surfactant-free coreduction route at 298 K. Typically, 29.1 mg of $\text{NiCl}_2 \cdot 6\text{H}_2\text{O}$ and 22.5 mg of $\text{FeSO}_4 \cdot 7\text{H}_2\text{O}$ were firstly dissolved in 3.5 mL of water, meanwhile, $\text{Na}_2\text{MoO}_4 \cdot 2\text{H}_2\text{O}$ (48.9 mg) was dissolved in 0.5 mL of water. The reason of separately dissolution is to minimize the formation of MoO_3 precipitate, which may form by the reaction between acidic NiCl_2 , FeSO_4 and alkaline Na_2MoO_4 . Then, the above two solutions were simultaneously added into 1mL aqueous solution containing NaBH_4 (30 mg) with magnetic stirring until the bubble generation ceased and finally the black product of $\text{Ni}_{0.6}\text{Fe}_{0.4}\text{Mo}$ could be obtained.

The system of $\text{Ni}_{0.6}\text{Fe}_{0.4}\text{Mo}_x$ NPs with different molar contents of Mo ($x = 0, 0.25, 0.5, 0.75, 1$ and 1.25) were also prepared as the above method by changing the addition content of $\text{Na}_2\text{MoO}_4 \cdot 2\text{H}_2\text{O}$. While for the synthesis of $\text{Ni}_y\text{Fe}_{1-y}\text{Mo}$ NPs, the molar ratio of Ni/Fe was changed from 0 to 1 ($y = 0, 0.2, 0.4, 0.6, 0.8$ and 1), when keeping the molar ratio of $(\text{Fe} + \text{Ni})/\text{Mo}$ as a constant of 1.

Catalytic activities: Typically, catalytic reactions were carried out using a two-necked round bottom flask which contained an aqueous suspension of the as-prepared $\text{Ni}_{0.6}\text{Fe}_{0.4}\text{Mo}$ nanocatalysts ($n_{\text{Ni}+\text{Fe}+\text{Mo}}=0.4$ mmol, 5 mL). One neck of the flask was connected to a gas burette and the other was connected to a pressure-equalization funnel to introduce 4 mL of solution containing $\text{N}_2\text{H}_4 \cdot \text{H}_2\text{O}$ (0.5 M) and NaOH (1.8 M). The catalytic reaction was started when the hydrazine aqueous solution was added into the catalyst suspension in the flask with magnetic stirring. The evolution of gas was monitored using the gas burette. The reaction was carried out at 323 K under ambient atmosphere.

The catalytic activities of other catalysts for $\text{N}_2\text{H}_4 \cdot \text{H}_2\text{O}$ decomposition were also applied as the above method. The molar ratios of $\text{NiFe}/\text{N}_2\text{H}_4 \cdot \text{H}_2\text{O}$ for all the catalytic

reactions were kept as a constant of 0.1. The reactions over $\text{Ni}_{0.6}\text{Fe}_{0.4}\text{Mo}$ were carried out at different temperatures (298, 303, 308, 313, 318 and 323 K) to evaluate the activation energy for decomposition of $\text{N}_2\text{H}_4\cdot\text{H}_2\text{O}$ in aqueous solution under ambient atmosphere.

Moreover, in order to exclude the effects of magnetic property on the catalytic performance upon the N_2H_4 decomposition, the hydrogen generation reaction from N_2H_4 aqueous solution by shaking instead of magnetic stirring has also been applied at 323 K.

Recycle stability: After the $\text{N}_2\text{H}_4\cdot\text{H}_2\text{O}$ decomposition reaction over $\text{Ni}_{0.6}\text{Fe}_{0.4}\text{Mo}$ was completed, another equivalent of $\text{N}_2\text{H}_4\cdot\text{H}_2\text{O}$ (0.5 M, 4 mL) was subsequently introduced into the flask to regenerate H_2 at 323 K under ambient atmosphere. The evolution of gas was monitored by using the gas burette.

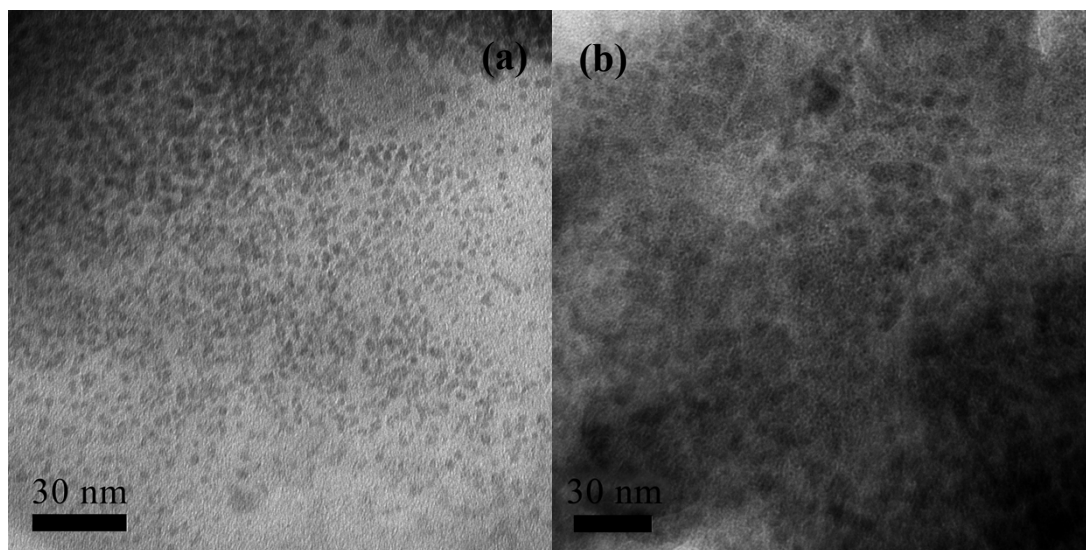


Fig. S1 TEM images of the as-synthesized (a) $\text{Ni}_{0.6}\text{Fe}_{0.4}\text{Mo}$ and (b) $\text{Ni}_{0.6}\text{Fe}_{0.4}$ NPs.

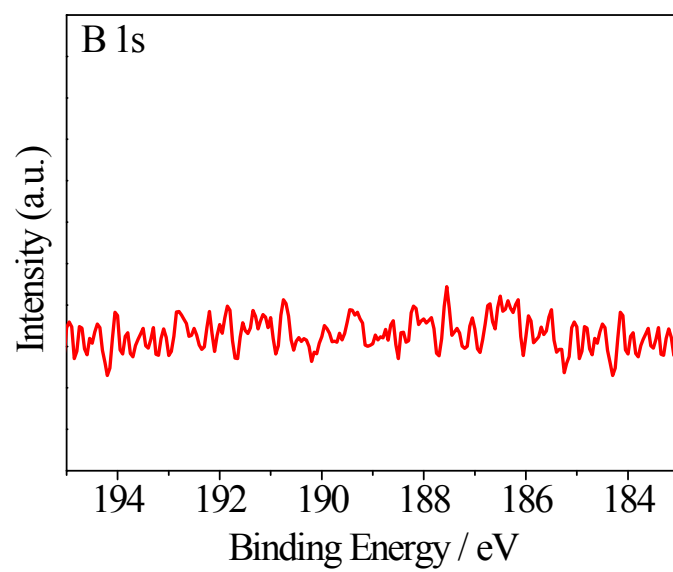


Fig. S2 XPS spectrum of B 1s for the $\text{Ni}_{0.6}\text{Fe}_{0.4}\text{Mo}$ catalyst.

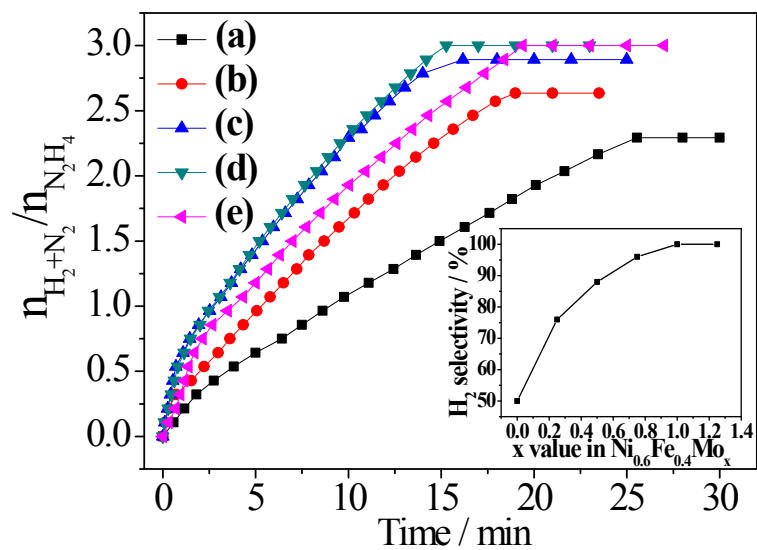


Fig. S3 Time-course plots for the decomposition of $N_2H_4 \cdot H_2O$ aqueous solution (0.5 M, 4 mL) to H_2 catalyzed by $Ni_{0.6}Fe_{0.4}Mo_x$ NPs (a) $x = 0.25$, (b) 0.5, (c) 0.75, (d) 1.0 and (e) 1.25 ($n_{Ni+Fe}/n_{N_2H_4} = 0.1$) with NaOH (7.2 mmol) at 323 K.

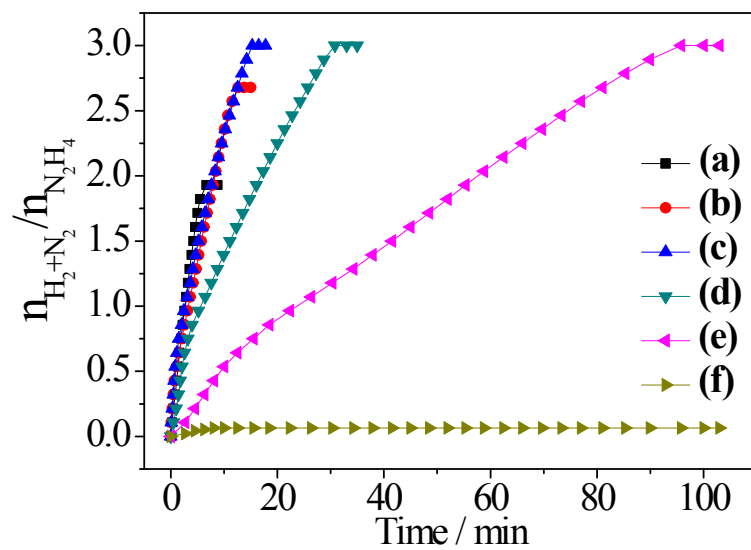


Fig. S4 Time-course plots for the decomposition of $\text{N}_2\text{H}_4 \cdot \text{H}_2\text{O}$ aqueous solution (0.5 M, 4 mL) to H_2 catalyzed by $\text{Ni}_{1-y}\text{Fe}_y\text{Mo}$ NPs (a) $y = 0$, (b) $y = 0.2$, (c) $y = 0.4$, (d) $y = 0.6$, (e) $y = 0.8$ and (f) $y = 1$ ($n_{\text{Ni}+\text{Fe}+\text{Mo}}/n_{\text{N}_2\text{H}_4} = 0.2$) with NaOH (7.2 mmol) at 323 K.

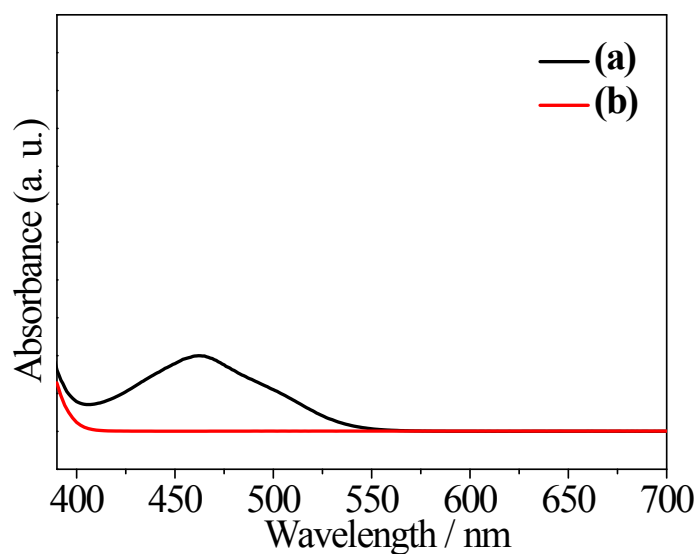


Fig. S5 UV-Vis spectra of hydrous hydrazine (a) before and (b) after the completion of hydrazine decomposition reaction over the $\text{Ni}_{0.6}\text{Fe}_{0.4}\text{Mo}$ nanocatalysts.

It can be seen from Figure S5a† that, before the catalytic reaction, there is a characteristic adsorption peak at 458 nm, which is attributed to the hydrazine and yellow resultant of paradimethylaminobenzaldehyde (PDAB) and in acid solution.^{S1} While after the reaction, the peak at 458 nm disappeared (Fig. S5b†), indicating the full decomposition of $\text{N}_2\text{H}_4 \cdot \text{H}_2\text{O}$ over catalyst of $\text{Ni}_{0.6}\text{Fe}_{0.4}\text{Mo}$.

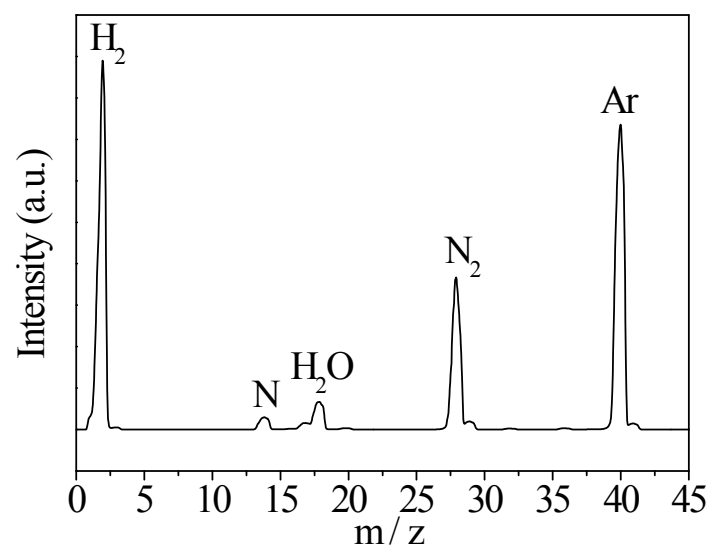


Fig. S6 Mass spectra of released gases from the complete decomposition of hydrazine catalyzed $\text{Ni}_{0.6}\text{Fe}_{0.4}\text{Mo}$ NPs in argon at 323 K.

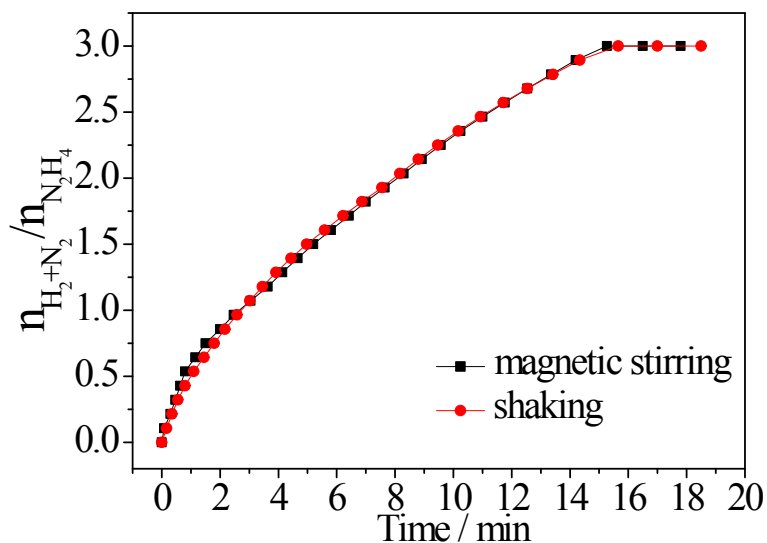


Fig. S7 Time-course plots for the decomposition of $N_2H_4 \cdot H_2O$ aqueous solution (0.5 M, 4 mL) to H_2 catalyzed with NaOH (7.2 mmol) over $Ni_{0.6}Fe_{0.4}Mo$ ($n_{Ni+Fe+Mo}/n_{N_2H_4}=0.2$) catalyst by magnetic stirring and shaking at 323 K under ambient atmosphere.

As shown in Fig. S7, the catalytic activities of $Ni_{0.6}Fe_{0.4}Mo$ for decomposition of $N_2H_4 \cdot H_2O$ by magnetic stirring and shaking show no obvious difference, which means that magnetic stirring has no negative impact on the performance of the $Ni_{0.6}Fe_{0.4}Mo$ catalyst. This may due to the small amount of Ni or Fe and the uniform dispersion of the as-prepared tiny NPs.

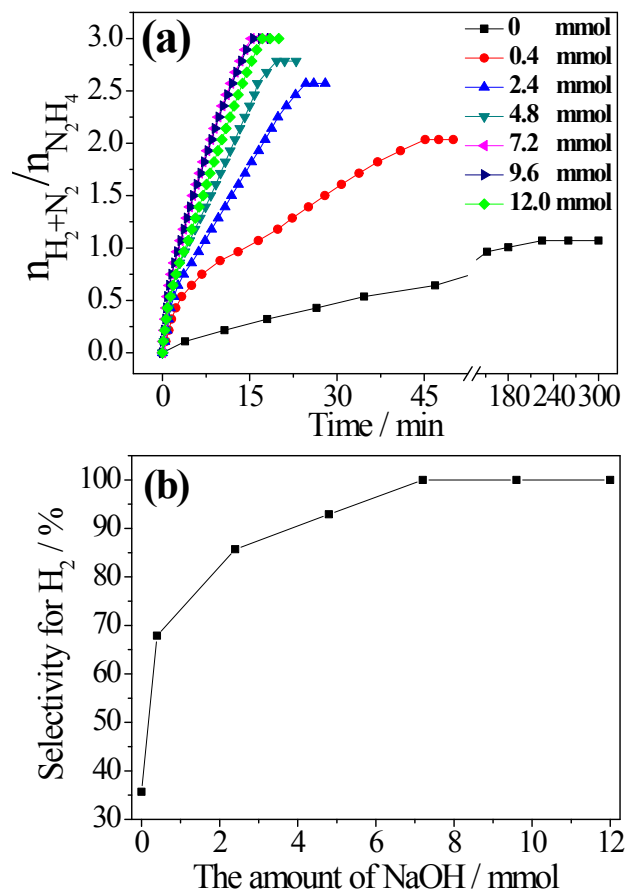


Fig. S8 (a) Decomposition of $N_2H_4 \cdot H_2O$ (0.5 M, 4 mL) catalyzed by $Ni_{0.6}Fe_{0.4}Mo$ ($n_{Ni+Fe+Mo}/n_{N_2H_4}=0.2$) with different amounts of NaOH at 323 K under ambient atmosphere and (b) the according selectivity for H_2 .

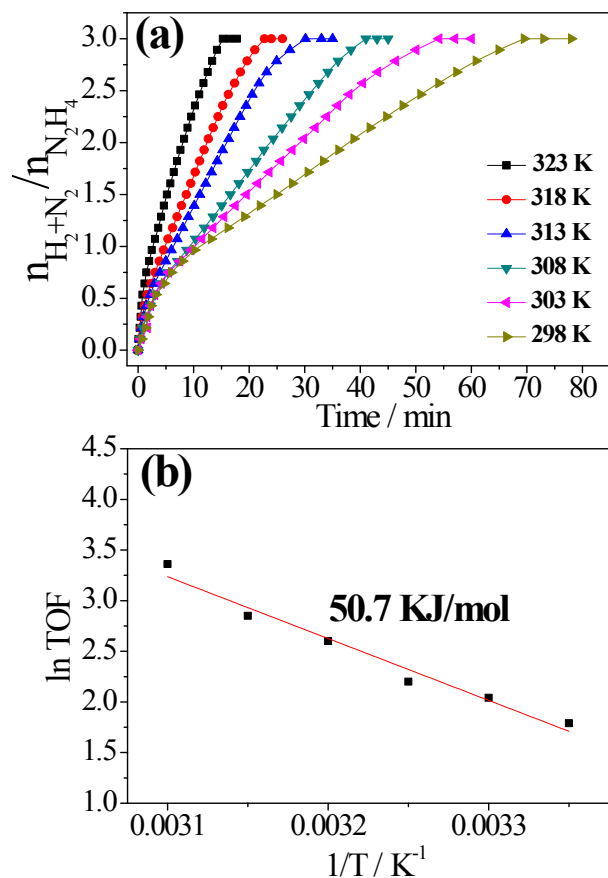


Fig. S9 (a) Time-course plots for the decomposition of $N_2H_4 \cdot H_2O$ aqueous solution (0.5 M, 4 mL) to H_2 catalyzed by $Ni_{0.6}Fe_{0.4}Mo$ ($n_{Ni+Fe+Mo}/n_{N_2H_4}=0.2$) at different temperatures. (b) Arrhenius plots for decomposition of hydrazine catalyzed by $Ni_{0.6}Fe_{0.4}Mo$ NPs.

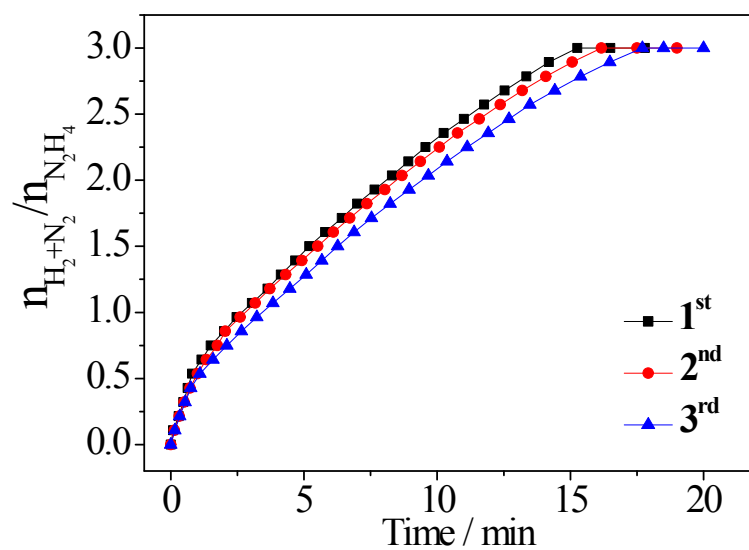


Fig. S10 Lifetime test of the $\text{Ni}_{0.6}\text{Fe}_{0.4}\text{Mo}$ nanocatalyst ($n_{\text{Ni+Fe+Mo}}/n_{\text{N}_2\text{H}_4}=0.2$) toward the decomposition of hydrazine (0.5 M, 4 mL) with NaOH (7.2 mmol) at 323 K under ambient atmosphere.

Table S1. Activities in terms of TOF values of different nanocatalysts tested in hydrogen generation from the decomposition of N_2H_4 aqueous solution.

Catalyst	Temp (K)	Reaction time (h)	Volume of gas (mL)	n_{catalyst} (mmol)	Selectivity for H_2 (%)	TOF _{initial} (h^{-1})
$\text{Ni}_{0.95}\text{Ir}_{0.05}$	298	6.500	136	0.197	100	2.2 [15]
$\text{Ni}/\text{Al}_2\text{O}_3$	303	1.167	103	0.661	93	2.2 [27]
Rh	298	3.000	68	0.197	43.8	2.5 [10]
$\text{Ni}_{0.93}\text{Pt}_{0.07}$	298	3.167	136	0.264	100	2.8 [14]
$\text{Rh}_{10}\text{Ni}_{90}$	323	4.500	136	0.200	100	3.3 [16]
$\text{Ni}_{0.60}\text{Pd}_{0.40}$	323	3.167	113	0.197	82	3.8 [12]
NiFe ($n_{\text{Ni}}/n_{\text{Fe}} = 1:1$)	343	3.167	138	0.200	100	4.2 [26]
Rh_4Ni	298	2.667	136	0.246	100	4.8 [11]
$\text{Ni}_{1.5}\text{Fe}_{1.0}\text{-alloy}/(\text{MgO})_{2.5}$	299	0.967	104	0.16	94	10.3 [29]
$\text{Cu}@ \text{Fe}_5\text{Ni}_5$	343	1.000	138	0.22	100	11.9 [31]
$\text{NiIr}_{0.059}/\text{Al}_2\text{O}_3$	303	0.258	109	0.645	99	12.4 [19]
$\text{Ni}_{64.1}\text{Mo}_{11.5}\text{B}_{24.4}\text{-La}(\text{OH})_3$	323	0.258	138	0.6	100	13.3 [28]
$\text{RhNi}@ \text{graphene}$ ($n_{\text{Rh}}/n_{\text{Ni}} = 4.4:1$)	298	0.817	138	0.244	100	13.7 [13]
$\text{NiPt}_{0.057}/\text{Al}_2\text{O}_3$	303	0.192	109	0.583	99	16.5 [17]
NiFe/Cu ($n_{\text{Ni}}/n_{\text{Fe}}/n_{\text{Cu}} = 1:1:2$)	343	0.283	138	0.4	100	17.6 [30]
$\text{Ni}_{0.9}\text{Pt}_{0.1}/\text{Ce}_2\text{O}_3$	298	0.717	172	0.250	100	28.1 [18]
$\text{Ni}_{0.6}\text{Fe}_{0.4}\text{Mo}$	323	0.250	140	0.4	100	28.8[This study]
$\text{Ni}_{0.8}\text{Pt}_{0.2}@ \text{ZIF-8}$	323	0.433	69	0.067	100	45 [22]
$\text{Ni}_{0.90}\text{Pt}_{0.05}\text{Rh}_{0.05}/\text{La}_2\text{O}_3$	298	0.300	172	0.250	100	45.9 [24]
$\text{Co}_{0.65}\text{Pt}_{0.30}(\text{CeO}_x)_{0.05}$	298	0.058	124	0.250	72.1	194.8 [23]

Table S2. Activities in terms of TOF values of recycle test (3 times) of hydrogen generation from the decomposition of N₂H₄ (0.5 M, 4 mL) aqueous solution with Ni_{0.6}Fe_{0.4}Mo nanocatalysts ($n_{Ni+Fe+Mo}/n_{N_2H_4}=0.2$).

Catalyst	Recycle number	Temp. (K)	Reaction time (h)	Volume of gas (mL)	n _{catalyst} (mmol)	Selectivity for H ₂ (%)	TOF _{initial} (h ⁻¹)
Ni _{0.6} Fe _{0.4} Mo	1 st	323	0.254	140	0.4	100	28.8
Ni _{0.6} Fe _{0.4} Mo	2 nd	323	0.269	140	0.4	100	27.2
Ni _{0.6} Fe _{0.4} Mo	3 rd	323	0.295	140	0.4	100	23.9

Calculation methods:

$$\text{TOF}_{\text{initial}} = \frac{P_{\text{atm}} V_{\text{H}_2+\text{N}_2} / RT}{3n_{\text{metal}} t} \quad (\text{S1})$$

Where $\text{TOF}_{\text{initial}}$ is the initial turnover frequency, P_{atm} is the atmospheric pressure, $V_{\text{H}_2+\text{N}_2}$ is the volume of the generated gas (H_2+N_2) when the conversion reaches 50%, R is the universal gas constant, T is the room temperature (298 K), n_{metal} is the mole number of metal catalyst, and t is the reaction time when the conversion reaches 50%.

The relationship of the temperature and the initial rate (conversion <50%)^{S2} was followed Arrhenius behavior. The Arrhenius' reaction rate equation can be written as follows:

$$\ln \text{TOF} = \ln A - E_a / RT \quad (\text{S2})$$

Where A is the reaction constant.

References:

- S1. L. Yu, X. S. Zhang and L. Y. Yu, *Adv. Mater. Res.* 2012, **396-398**, 130.
- S2. A. Boddien, D. Mellmann, F. Gärtner, R. Jackstell, H. Junge, P. J. Dyson, G. Laurenczy, R. Ludwig and M. Beller, *Science*, 2011, **333**, 1733.